

A Connection Between Star Formation Rate and Dark Matter Halos at $Z \sim 6$ In 2013 Planck Cosmology.

F.L. Gómez-Cortés¹

Departamento de Física, Universidad de los Andes, Colombia

Received _____; accepted _____

ABSTRACT

This work relates baryonic matter and dark matter at redshift $z = 5.9$ using observational data from CFHTLS (Willott et al. 2013), HUDF09 (Bouwens 2006, 2012), UKIDSS and SDXS (McLure et al. 2009), and results of the Multidark Simulation (Riebe 2013) in a cubic box of 1000Mpc h^{-1} length with 2013 Planck Cosmology. The Luminosity Function (LF) is fitted via four parameters with the Markov Chain Monte Carlo method. The relationship between the Dark Matter Halos Mass and Star Formation Rate is obtained using the relationship between the UV continuum (from the fitted LF) and Star Formation Rate (SFR) by Kennicutt (1998). Cosmic variance effects are studied on smaller boxes of 250Mpc h^{-1} length.

Halos.

Subject headings: Dark Matter, LF, SFR, High Redshift Galaxies, Reionization

1. Introduction

Cosmological simulations still playing an important role on astrophysics and cosmology. They have become the bridge between observations and theory, a laboratory where is possible to create universes with different parameters and new physics.

This is an important tool in the study of dark matter. Since its existence was purposed, DM has been not observed directly neither on telescopes or high energy particle colliders, there exists many other theories explaining the observed universe behavior modifying the gravity itself.

The most successful and accepted cosmological model is the Lambda-CDM. Dark matter is a significative component of the universe. (Trimble 1987)

Hierarchy Structure Evolution: Early formation of small structures merging on major structures after.

From simulations, Halo Mass Function as function of redshift (or time).

In this paper is established a relation between dark matter and galaxy luminosity functions at high redshift. This relation is a direct connection between the Lambda-CDM model and the farthest galaxy observations made with space and grounded telescopes.

Star formation rate as function of time. Peak at $z \sim 2$.

“An important frontier in the study of very high redshift galaxies remains the study of their stellar populations. Galaxies within a few hundred million years of the Big Bang are expected to be quite different from galaxies at lower redshift, with significantly younger ages and lower metallicities. For very young and chemically immature systems, changes in the stellar population could include a transition to a more top-heavy IMF (e.g., Bromm & Larson 2004), evolution in the dust composition (e.g., due to changes in the dust production

mechanism: Maiolino et al. 2004), as well as a much lower dust extinction overall (e.g., Bouwens et al. 2009; Finlator et al. 2011; Dayal & Ferrara 2012).” BOWENS 2014 BETA SLOPE

Main Objective: Reproduce the observed luminosity function at redshift $z = 5.9$ from a DMH catalog from simulations.

This paper is organized as follows: In section 2... in section 3...

1.1. Halo Mass Function (HMF)

1.2. Cosmic Variance

“One of the most fundamental properties of galaxy sub- populations at any epoch is their number density. However, observational estimates of galaxy number densities in finite volumes are subject to uncertainty due to cosmic variance, arising from underlying large-scale density fluctuations and leading to uncertainties in excess of naive Poisson errors. Note that this source of uncertainty is referred to as sample variance in other branches of cosmology. For sampling vol- umes much larger than the typical clustering scale of the observed objects, cosmic variance is not significant.” A COSMIC VARIANCE COOKBOOK

“However many important existing surveys have a sampling volume that is small enough that cosmic variance may dominate the un- certainties. This may be particularly true at high redshift, where galaxies are expected to be much more strongly clus- tered than dark matter (Kauffmann et al. 1999; Baugh et al. 1999; Coil et al. 2004; Moster et al. 2009). Still, many pub- lished quantities which are based on number density (e.g. lu- minosity functions, stellar mass functions, etc.) are quoted with error budgets that do not properly account for cosmic variance. As shown by Trenti & Stiavelli (2008), the normal- ization and the slope of high-redshift luminosity functions can be affected by cosmic

variance errors.” A COSMIC VARIANCE COOKBOOK

“Somerville et al. (2004) provided predictions that could be used to estimate cosmic variance as a function of mean red- shift and survey volume, using the number density of the pop- ulation to estimate the bias, assuming one galaxy per halo.” A COSMIC VARIANCE COOKBOOK

=====lllllllll COSMIC VARIANCE CALCULATOR iiiiiiiii=====

Results obtained using CosmicVarianceCalculator v1.02 Developed by Michele Trenti & Massimo Stiavelli If you use these results in scientific papers, please refer to: Trenti & Stiavelli (2008), ApJ, 676, 767

2. Linking Galaxy Luminosity Function (GLF) and Dark Matter Halo (DMH) mass

READ THIS PAPER Vale - Ostriker arXiv:astro-ph/0402500v2 6 Jul 2004 Mon. Not. R. Astron. Soc. Linking halo mass to galaxy luminosity

“In recent years, N-body numerical simulations have given us a good understanding of dark matter structure for standard cosmological scenarios, while large scale observational surveys have done the same for the distribution of galaxies” arXiv:0402500v2

“More indirect approaches have also been studied. The halo occupation distribution (HOD) model (Seljak 2000; Benson 2001; Bullock, Wechsler, & Somerville 2002; Zheng et al. 2002; Berlind & Weinberg 2002; Berlind et al. 2003; Magliocchetti & Porciani 2003) is based on the prob- ability $P(N|M)$ that a halo of mass M is host to N galax- ies. By specifying the $P(N|M)$ function, along with some form for the distribution of dark matter and galaxies within each halo, it is then possible to relate different statistical indicators of the dark matter and galaxy distributions, such as correlation functions, to each other.

This fully specifies the bias between the galaxy and the underlying matter distributions.
” arXiv:0402500v2

“Other authors have used a slightly different method. Instead of trying to specify the number of galaxies in each halo, they treat the halo as a whole and identify it with a galaxy group. Then, by comparing the group luminosity function with the halo mass function, they obtain the luminosity associated with each halo (Peacock & Smith 2000; Marinoni & Hudson 2002), ” arXiv:0402500v2

=====lllllllll Check Peacock & Smith 2000; Marioni & Hudson 202

2.1. Magnitude to Luminosity

Luminosity Functions (LF) are usually expressed in terms of magnitude instead luminosity. Luminosity is the energy emitted by a source in a given wavelength range, is a physical quantity. Magnitude is a classification inherited from ancient Greeks, this quantifies the response of the first astrometric device: the human eye, this perception grows logarithmically with the retrieved radiation.

Luminosity of any object can be compared with Sun Luminosity ($L_{\lambda\odot}$) at any wavelength. With the Sun Magnitude as reference ($M_{\lambda\odot}$), the absolute magnitude of the object at a specific wavelength is given by:

$$M_{\lambda} = M_{\lambda\odot} - 2.5 \log_{10} \left(\frac{L_{\lambda}}{L_{\lambda\odot}} \right)$$

The solar absolute magnitude in the U filter is $M_{U\odot} = 5.61$, and the solar luminosity in the same filter is $L_{U\odot} = 10^{18.48} \text{ergs s}^{-1} \text{Hz}^{-1}$ or $L_{U\odot} = 3.02 \times 10^{18} \text{ergs s}^{-1} \text{Hz}^{-1}$. The solar luminosity can be used as reference unit, in this fashion, the typical luminosity of a galaxy can be expressed in terms of $10^8 - 10^{11}$ times the sun luminosity.

The absolute magnitude of a galaxy equation in the U filter:

$$M_U = 51.82 - 2.5 \log_{10}(L_U)$$

2.2. The Luminosity Model

In this model we have made two assumptions:

1. Each halo in the catalog hosts one galaxy. There are not empty halos, also none of halos has two or more galaxies.
2. The UV luminosity of each galaxy is function of one variable: the mass of the DMH in wich is located.

The simplest relation we can have is a powerlaw:

$$L = L_0 M^\alpha \tag{1}$$

but has not well agreement with observed luminosity functions.

A better model is a four parameter function. Each galaxy has a luminosity given by:

$$L = L_0 M \left[\left(\frac{M}{M_0} \right)^{-\beta} + \left(\frac{M}{M_0} \right)^\gamma \right]^{-1} \tag{2}$$

where M is the hosting DMH mass, L_0 is a normalization constant, M_0 is the critical mass where the luminosity function has a slope change, β and γ are the slopes. This equation has a similar fashion to the mass to light relation (van den Bosch 2003) and the mean relation between stellar mas of a galaxy and the mas of its halo used by Moster (2010).

There are more complex models(Lee 2009) that includes a random behavior: galaxies has not synchronization on the beginning of star forming stage, also this stage may be time limited. This is called duty cycle. It is probable to have in the observations some invisible galaxies in the UV continuum due their duty cycle may has not started as well it may ended. Also may be present a normal distribution of the luminosity around the expected values.

2.3. Star Formation Rate

The age of a star can be estimated by analyzing its spectrum. But when far galaxies are studied, individual stars can not be resolved. Is not possible to make a detailed census of the galaxy population. Only is possible to get information from the whole stellar population, an integrated spectrum.

There is a method(Madau 1998) in wich a linear relation between SFR and luminosity in specific wavelength ranges can be assumed. This model allows to estimate the young stars fraction and the mean SFR over periods of $10^8 - 10^9$ yr(Kennicutt 1998). The luminosity in the model, comes from the UV and the FIR broadband, also from specific recombination lines.

In a typical galaxy spectrum the visible wavelengths are dominated by the main sequence stars (A to early F) and G-K giants. In few wavelength ranges we have a significative contribution from the young stars rather than the old stars. The infrared and far infrared wavelengths emission is dominated by dust, this dust is heated by the whole stellar population, in particular by young, UV-bright stars (Law 2011).

On active galaxies the UV broadband emission is dominated by late-O and early-B type stars, with temperature near to 40.000K. These hot and massive stars has a lifetime below 10^7 Gyr, they spend their nuclear fuel faster than smaller and cooler sunlike stars.

The relation between UV luminosity and Star Formation Rate (Madau 1998; Kennicutt 1998) is given by:

$$\text{SFR} (M_{\odot}\text{yr}^{-1}) = 1.4 \times 10^{-28} L_{\nu} (\text{erg s}^{-1}\text{Hz}^{-1}) \quad (3)$$

With Initial Mass Function (IMF) between $0.1M_{\odot}$ and $100M_{\odot}$, in the range of $1250 - 2500\text{\AA}$

The star forming rate will be:

$$SFR = k \times L_0 M \left[\left(\frac{M}{M_0} \right)^{-\beta} + \left(\frac{M}{M_0} \right)^{\gamma} \right]^{-1} \quad (4)$$

The UV dust absorption (Kennicutt 2009) is not taken account in this work.

3. Observations

This paper is based on four main observational data sets from the Hubble Space Telescope and three ground-based telescopes. All $z \sim 6$ LBG candidates were discovered using the drop-out technique (Steidel 2003). All magnitudes are in AB system.

The data from the Hubble Space Telescope Legacy (HSTL) (Bouwens et al. 2014) is a compilation of observations since the installation of the Advanced Camera for Surveys (ACS) in 2002, through the near-infrared Wide Field Camera 3 (WFC3/IR) installed in 2009, up to 2012. The HST fields of view are: XDF, HUDF09-1, HUDF09-2, CANDELS-S/Deep, CANDELS-S/Wide, ERS, CANDELS-N/Deep, CANDELS-N/Wide, CANDELS-UDS, CANDELS-COSMOS and CANDELS-EGS, with areas of 4.7, 4.7, 4.7, 64.5, 34.2, 40.5, 62.9, 60.9, 151.2, 151.9 and 150.7 arcmin² respectively. The total area corresponds to ~ 0.7 deg² over five different lines of sight, reducing cosmic variance effects. Two cameras performed the observations: ACS and WFC3/IR, using $B_{435}V_{606}i_{814}z_{850}I_{814}Y_{098}Y_{105}J_{125}JH_{140}$ and H_{160} filters. The limit magnitude is between ~ 27.5 mag in CANDELS-EGS and ~ 30 mag in the deepest field (XDF). Total number of $z=6$ LBG candidates is 940, most of them in the faint end of the LF, magnitudes in the rest frame are in the range $-22.52 \leq M_{1600} \leq -16.77$. The Schechter parameters derived are: $\phi^*/\text{Mpc}^{-3} = (0.33^{+0.15}_{-0.10}) \times 10^{-3}$, $M_{1600}^* = -21.16 \pm 0.20$ and $\alpha = -1.91 \pm 0.09$. Bouwens et al. (2014) reported that using just few fields of view, UVLF has a slightly non-Schechter-like form.

Willott et al. (2013) presented the sixth release of the Canada-France-Hawaii Telescope Legacy Survey CFHTLS. The observations were performed over four separated fields covering a total area ~ 4 deg² (a large area), it gives this survey great robustness. Optical observations used MegaCam [CITE REQUIRED] with $u^*g'r'i'z'$ filters. The main selection criteria: all the objects must be brighter than magnitude $z' = 25.3$. The final number of LBGs founded was 40. Moreover, they get spectroscopic confirmation for 7 candidates

using GMOS spectrograph on the Gemini Telescopes, which has a $\ll 5.5$ -square arcmin field of view . They show incompleteness in the sample due to foreground contamination and the detection algorithm; there is no warranty to have every object brighter than the limit magnitude on the faint limit. The full galaxy LF at $z = 6$ cannot be obtained as in other studies. Nevertheless, this survey was focussed on the highly luminous LBGs. LF is calculated using the stepwise maximum likelihood method of Efstathiou et al. [MNRAS 1998 Cite required!!!], within magnitudes from $M_{1350} = -22.5$ up to -20.5 . The luminosity function of $z = 5.9$ shows an exponential decline at the bright end, where feedback processes and inefficient last cooling limit star forming in bright galaxies hosted in the most massive halos.

McLure et al. (2009) build the luminosity function for $z = 5$ and $z = 6$ using data from two ground-based telescopes: the United Kingdom Infrared Telescope in the near-IR imaging and Subaru Telescope for the optical imaging. They use the first data release of the UKIRT Infrared DeepSky Survey Ultra Deep Survey (UDS), together with the Subaru XMM-Newton Survey (SXDS). Total observed area is 0.63 deg^2 uniformly covered by booth catalogues. The UKIRT was equipped with the WFCAM using JK filters. The Subaru was equipped with the Suprime-Cam with the $BVRi'z'$ filters. All candidates where brighter than $z' = 26$. The UV rest frame magnitude range is $-22.4 \leq M_{1500} \leq -20.6$. The LF was calculated using the maximum likelihood estimator of Schmidt (1968). [Cite Required!!!!]. Their analysis gave a total number of 104 LBG candidates in the redshift range $5.7 \leq z \leq 6.3$. LF was parameterized according to the Schechter function with $\phi^*/\text{Mpc}^{-3} = (1.8 \pm 0.5) \times 10^{-3}$, $M_{1500}^* = -20.04 \pm 0.12$ and $\alpha = -1.71 \pm 0.11$.

The dataset was retrieved from McLure et al. (2009) graph using GAVO-DEXTER¹.

¹<http://dc.zah.uni-heidelberg.de/dexter/ui/ui/custom>

Finkelstein HST using CANDELS/GOODS fields, HUDF and Hubble Frontier Field deep parallel observations near the Abell 2744 and MACS J0416.1-2403 clusters. (Unlensed fields)

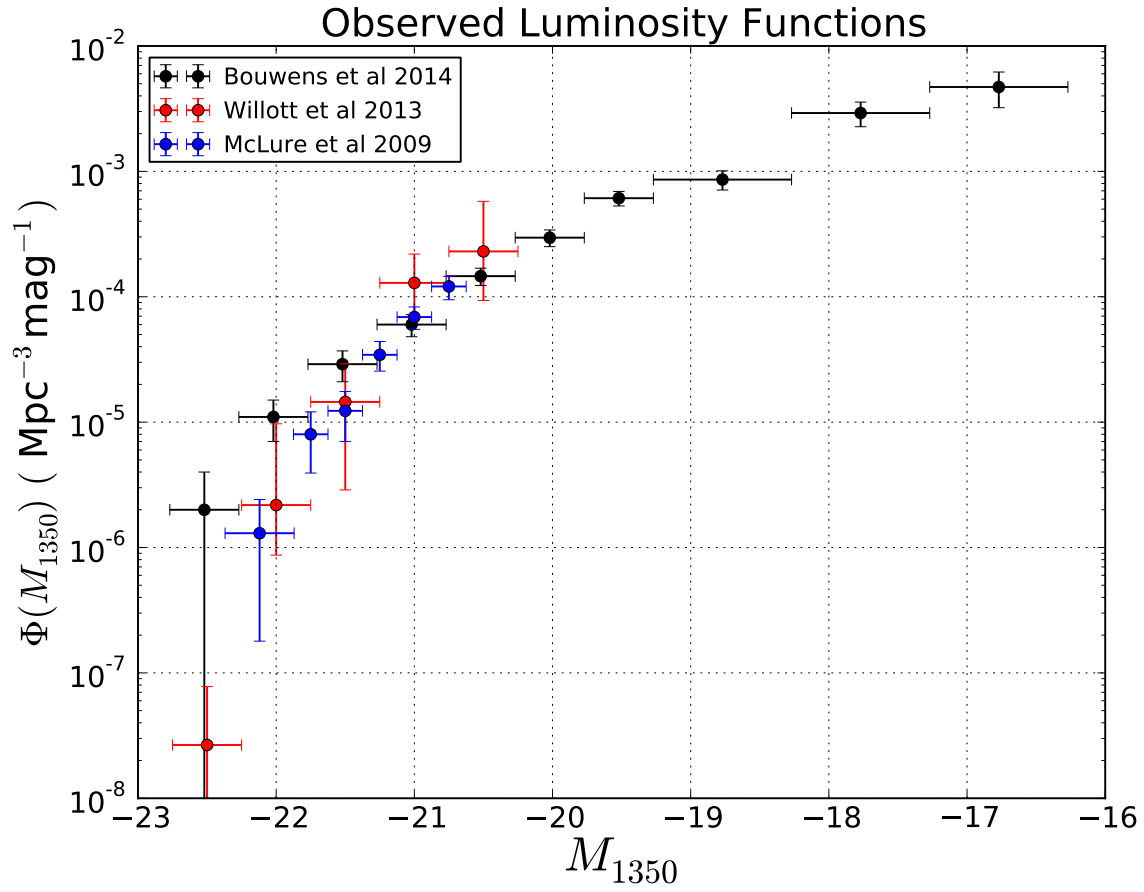


Fig. 1.— Observational data from Bouwens et al. (2014); McLure et al. (2009) and Willott et al. (2013).

4. Discussion

(Lundgren 2014(@) SFR evolution from $z = 1$ to 6

(Bouwens et al. 2014) HST Legacy

(Jiang 2011) Keck spectroscopy

“Fig. 16. Updated Determinations of the derived SFR (left axis) and U V luminosity (right axis) densities versus redshift (5.4). The left axis gives the SFR densities we would infer from the measured luminosity densities, assuming the Madau et al. (1998) conversion factor relevant for star-forming galaxies with ages of 108 yr (see also Kennicutt 1998). The right axis gives the U V luminosities we infer integrating the present and published LFs to a faint-end limit of 17 mag (0.03 L_{\odot})”BOUWENS 2014 UV LF

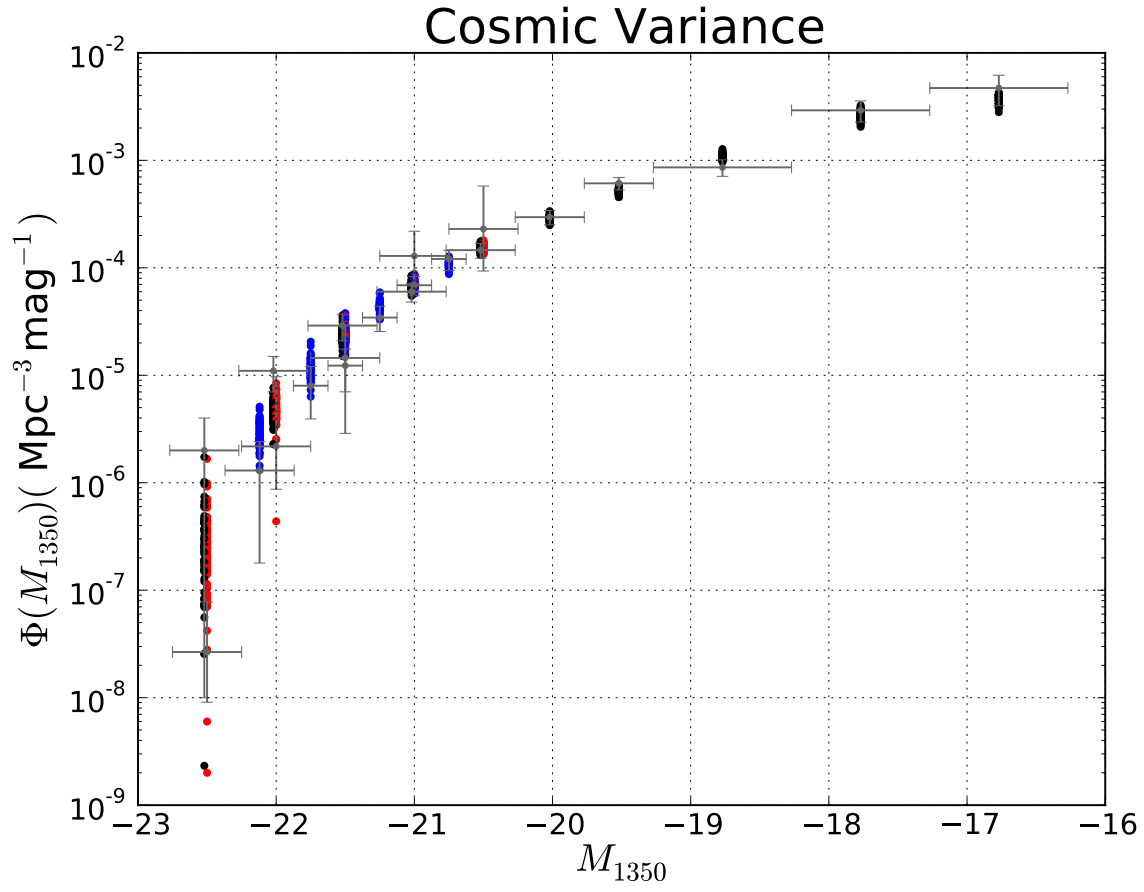


Fig. 2.— Cosmic Variance: The Luminosity Function is made using the DMH catalog from the full box and the set of parameters from the small boxes.

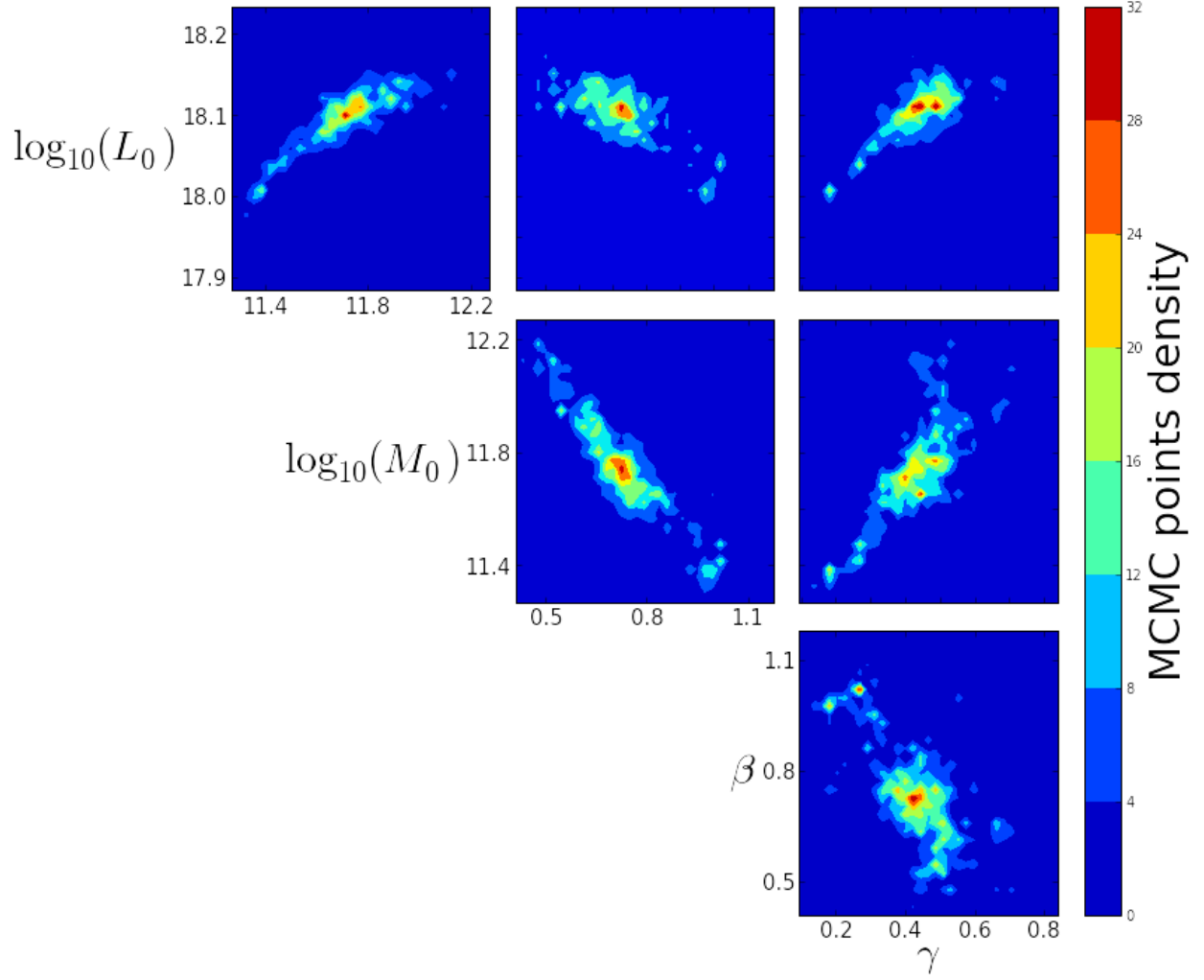


Fig. 3.— Covariance of parameters for one small box

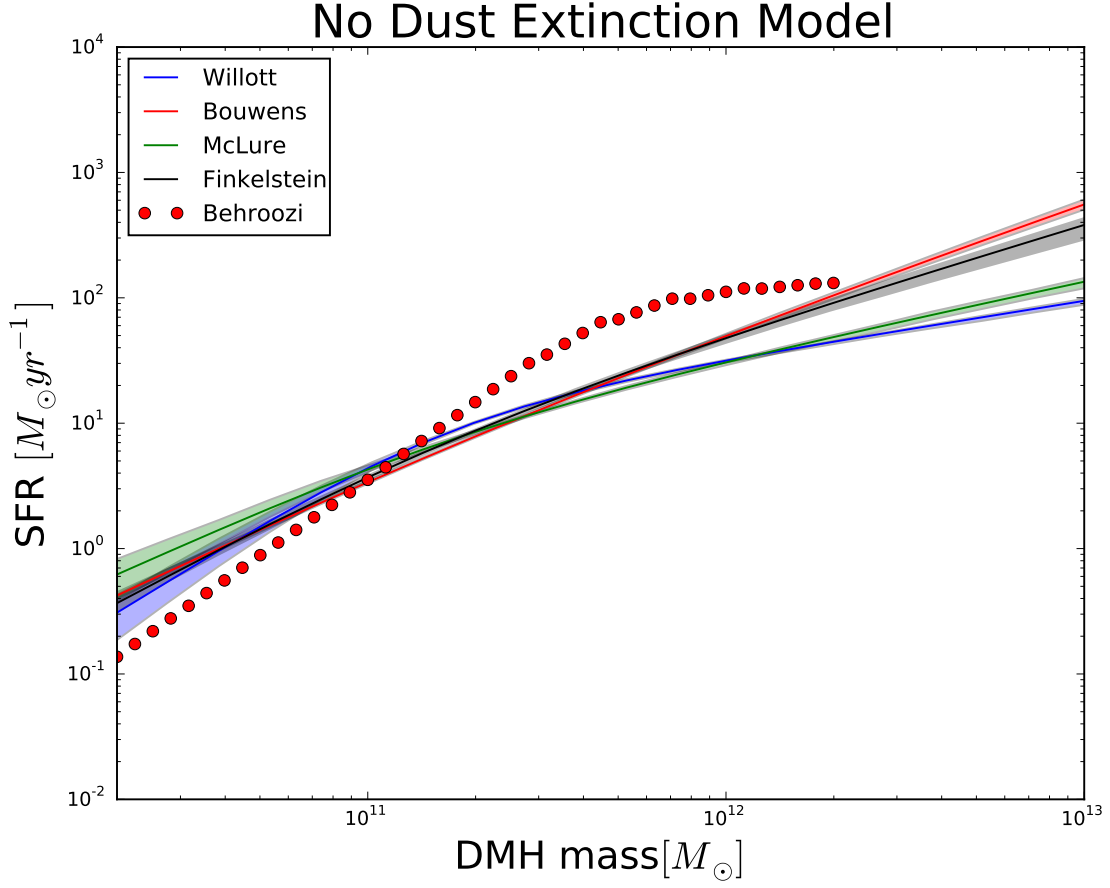


Fig. 4.— Star formation rate as function of the dark matter halo mass without dust attenuation. Solid lines represents the mean SFR value over the small boxes within 50% shaded region.

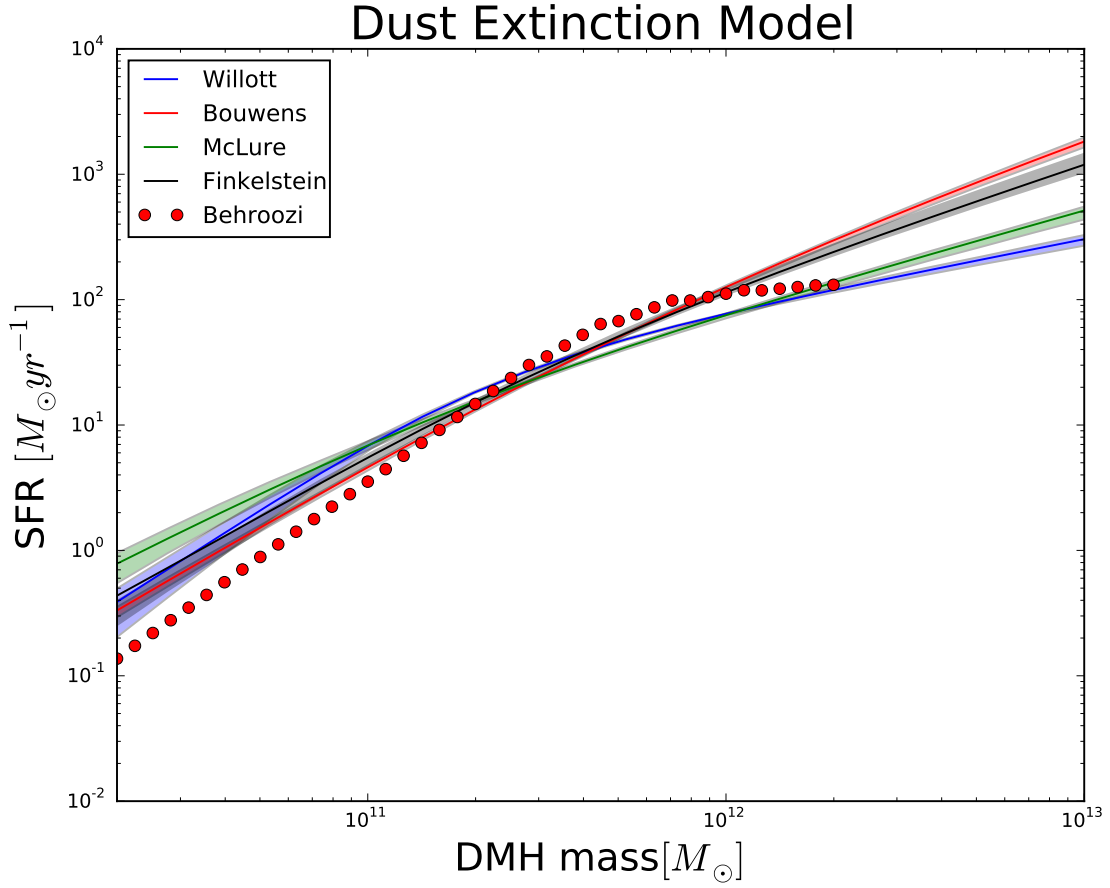


Fig. 5.— Star formation rate as function of the dark matter halo mass with dust attenuation. Solid lines represents the mean SFR value over the small boxes within 50% shaded region.

5. Summary

REFERENCES

- Bouwens, R. J. et al. 2006, ApJ, 653, 53
- Bouwens, R. J. et al. 2012, ApJ, 752, 5
- Bouwens, R. J., G. D. Illingworth, P. A. Oesch, M. Trenti, I. Labbé, L. Bradley, M. Carollo, et al. 2014, arXiv:1403.4295
- Kennicutt, Robert C., Jr. 1998, ARA&A, 36, 189
- Kennicutt, Robert C., Jr et al. 2009, ApJ, 703, 4672
- Law, K. et al. 2011, ApJ, 738, 124
- Jiang, Linhua et al. 2011, ApJ, 743, 65
- Lee, Kyoung-Soo et al. 2009, ApJ, 695, 368
- Lundgren, Britt F. et al, 2014, ApJ, 780, 34
- Madau, Piero. et al, 1998, ApJ, 498, 106M
- McLure, R. J., M. Cirasuolo, J. S. Dunlop, S. Foucaud, O. Almaini. 2009, MNRAS, 395, 2196
- Moster, Benjamin P. et al. 2010, ApJ, 710, 903
- Riebe, K. et al. 2013, AN, 334, 691
- Steidel, Charles C. et al. 2003, ApJ, 592, 728
- Tribble, Virginia. 1987, ARA&A, 25, 425
- van den Bosh, Frank C. et al. 2003, MNRAS, 40, 771

Willott, Chris J., Ross J. McLure, Pascale Hibon, Richard Bielby, Henry J. McCracken,
Jean-Paul Kneib, Olivier Ilbert, David G. Bonfield, Victoria A. Bruce, Matt J.
Jarvis. 2013, AJ, 145, 4